Chemical Physics Letters 671 (2017) 21–27

Contents lists available at ScienceDirect

Chemical Physics Letters

journal homepage: www.elsevier.com/locate/cplett

Research paper

A combined X-ray scattering and simulation study of halothane in membranes at raised pressures

N.L.C. McCarthy [a], N.J. Brooks [a,*], A.I.I. Tyler [a], Mohammad ElGamacy [b], P.R.L. Welche [c], M.C. Payne [c], P.-L. Chau [d,*]

[a] Department of Chemistry, Imperial College, London SW7 2AZ, UK
[b] Abteilung Proteinevolution, Max-Planck-Institut für Entwicklungsbiologie, 72076 Tübingen, Germany
[c] Theory of Condensed Matter Group, Cavendish Laboratory, Department of Physics, University of Cambridge, Cambridge CB3 0HE, UK
[d] Bioinformatique Structurale, CNRS URA 3528, Institut Pasteur, 75724 Paris, France

ARTICLE INFO

Article history:
Received 31 August 2016
In final form 16 December 2016
Available online 4 January 2017

Keywords:
X-ray scattering
Molecular dynamics simulations
Halothane
DMPC
General anaesthetics
Pressure reversal

ABSTRACT

Using a combination of high pressure wide angle X-ray scattering experiments and molecular dynamics simulations, we probe the effect of the archetypal general anaesthetic halothane on the lipid hydrocarbon chain packing and ordering in model bilayers and the variation in these parameters with pressure. Incorporation of halothane into the membrane causes an expansion of the lipid hydrocarbon chain packing at all pressures. The effect of halothane incorporation on the hydrocarbon chain order parameter is significantly reduced at elevated pressure.

1. Introduction

General anaesthetics (GAs) have been used for over 170 years, and millions of surgical procedures have been performed using these drugs, but their site and mechanism of action are still not entirely clear. In the beginning of the 20th century, Meyer [1] and Overton [2] attempted to rationalise the experimental findings, and proposed what is now known as the Meyer-Overton rule. It stated that the logarithm of the efficacy of an anaesthetic was proportional to the logarithm of its lipophilicity. Since this rule applied to a large variety of general anaesthetics, it suggested that a unified mechanism of action might exist.

Fifty years later, Johnson and Flagler [3,4] discovered the phenomenon of pressure reversal. They found that, by increasing ambient pressure to between 14 MPa and 21 MPa (140 and 210 bar), general anaesthesia by ethanol could be reversed in tadpoles. Paton and his co-workers [5,6] and Halsey and Wardley-Smith [7] extended the work by using several different anaesthetics and different animals, and the reversal phenomena were observed in all the general anaesthetics they used. The pressure where pressure reversal was observed depended on the species and the drug administered, and varied from 8 MPa (80 bar) [3] to 20 MPa (200 bar) [6]. This pressure reversal effect has since been observed in many species and using different kinds of general anaesthetics [8,9].

Subsequently, Trudell et al. [10,11] performed electron spin resonance experiments on spin-labelled phosphatidylcholine and halothane (1,1,1-trifluoro-2-chloro-2-bromo-ethane) solutions. They defined a bond order parameter S'_n based on the angular deviation, and found that applying halothane decreased S'_n but increasing pressure would increase S'_n. These results implied that the phospholipid cell membrane was involved in general anaesthetic action.

However, there is also significant evidence that a number of anaesthetic molecules act at specific protein binding sites. Several distinct protein targets have been identified and may be collectively contributing to the anaesthetic state. Among those are tandem-pore-domain potassium channels, NMDA receptors [12], voltage-gated sodium channels [13] and more importantly, anionic pentameric ligand-gated ion channels [14]. The latter class (especially the $GABA_A$ receptor) was subject to extensive studies aimed at identifying the location of the GAs binding site through targeted mutagenesis [15], mutagenesis and alkyl-labelling experiments [16], and modelling studies [17], where the binding site is thought

* Corresponding authors.
E-mail addresses: nicholas.brooks@imperial.ac.uk (N.J. Brooks), pc104@pasteur.fr (P.-L. Chau).

http://dx.doi.org/10.1016/j.cplett.2016.12.041
0009-2614/

to be located at the lipid-accessible side of the transmembrane domain.

Recently, Chau et al. [18,19] performed molecular dynamics simulations of a membrane patch with a concentration of halothane six times that of clinical concentration, and showed that the drugs aggregated inside the membrane at raised pressures. In a subsequent simulation system [20], the concentration of halothane used was only twice that of clinical concentration; they were able to show that there was aggregation at 20 MPa but not at 40 MPa. This effect was not observed in simulations involving another general anaesthetic, isoflurane (1,1,1-trifluoro-2-chloro-2-(difluoromethoxy)-ethane) [21].

Importantly, none of the currently suggested molecular mechanisms for anaesthetic action adequately explains the widely observed phenomenon of pressure reversal. The conformation and activity of membrane proteins (such as the $GABA_A$ ion channel which has been widely implicated in anaesthetic action) are known to be highly sensitive to the state of the membrane in which they are embedded [22,23]. Here, we have explored the combined effect of general anaesthetic incorporation and high pressure on the lipid hydrocarbon chains of model bilayer membrane systems. Using a combined experimental - simulation approach, we have been able to gain a unique insight into the changes in packing and conformational order of the lipid molecules.

2. Materials and methods

2.1. Experimental materials

DMPC (1,2-dimyristoyl-*sn*-glycero-3-phosphocholine) was purchased from Avanti Polar Lipids (>98% purity, Alabaster, AL, USA) and was used without further purification. Halothane was purchased from Sigma Aldrich (Gillingham, UK).

2.2. High-pressure X-ray scattering experiments

Dry samples of DMPC were hydrated with MilliQ water (60 wt %) and subjected to at least 10 freeze–thaw-vortex cycles. For anaesthetic containing samples, halothane was added to give a molar ratio of 128:80 lipid to halothane (representing a halothane concentration approximately 12 times greater than that of a clinical concentration [24]) and mixed thoroughly immediately prior to being loaded into sealed sample holders to minimise the effect of halothane evaporation. Samples were then mounted in a custom-built high pressure cell and subjected to a minimum of two pressure cycles (0.1–100 MPa) before each experiment to ensure sample homogeneity. Full details of the pressure cell used for X-ray studies have been described previously [25]. Briefly, the cell consists of a high tensile strength stainless steel body with 1-mm thick, 5-mm diameter sapphire windows. These windows provide good X-ray transmission (at 18 keV) while offering excellent pressure stability. Wide-angle X-ray scattering (WAXS) experiments were carried out at beamline I22 at Diamond Light Source in the range 0.1–100 MPa (1–1000 bar) at 310 K. The resulting two-dimensional WAXS patterns were radially integrated to give one-dimensional scattering intensity profiles. For each pressure measured, a water scattering pattern was recorded and used for baseline subtraction. Gaussian functions were fitted to peaks in the WAXS patterns to find the peak centres (most patterns showed only a single broad peak). The real space d-spacing (d) corresponding to the peak centres was calculated as $1/S$, where $S = \sin\theta/\lambda$ (where 2θ is the angle between the incident and scattered X-ray beams and λ is the X-ray wavelength). The maximum of the broad wide angle scattering peak indicates the average alkyl chain separation within the bilayer.

2.3. Molecular dynamics simulations

All molecular dynamics simulations were performed using NAMD version 2 [26], using the CHARMM36 potential [27] for the membrane, the TIP3P potential [28] for water, and a special potential for halothane [29], using the second set of partial charges. The initial configuration of hydrated DMPC membranes came from the web-based CHARMM-GUI membrane builder [30]. This system, under periodic boundary conditions, contains 64 DMPC molecules and is fully hydrated with 2048 water molecules. For anaesthetic containing simulations, 33 halothane molecules were added, resulting in approximately ten times clinical concentration of the drug. The halothane molecules were placed randomly in the simulation box, using the soft-core potential function implemented in NAMD.

For the pure DMPC system, molecular dynamics simulations were carried out with timesteps of 2 fs, at a temperature of 310 K and at a pressure of 0.1 MPa (1 bar). Langevin dynamics were applied; the thermostat was initially set with a time constant of 0.1 ps^{-1}, but this was reduced to 0.05 ps^{-1} over the course of equilibration (varying from 60 ns to 90 ns, depending on the pressure). The barostat was initially set with a piston decay time of 1 ps and a piston period of 2 ps, but these were increased during equilibration to a piston decay time of 500 ps and a piston decay period of 1 ns. The van der Waals cut-off was 12 Å, and Ewald summation was applied to electrostatic interactions. Data collection was carried out for 20 ns; configurations were output every 20 ps.

For the halothane-DMPC system, 33 halothane molecules were added to the membrane of 64 DMPC molecules. Post-insertion, the halothane-DMPC system was equilibrated for 200 ns. Subsequently, separate equilibration simulations (from 50 ns to 100 ns, depending on the pressure) were carried out at, respectively, 0.1 MPa (1 bar), 20 MPa (200 bar) and 40 MPa (400 bar). The piston decay time was increased to 0.5 ns and the piston decay period was increased to 1 ns. Data collection was carried out for 20 ns for both systems; configurations were output every 20 ps.

The structure factor was calculated as a function of the scattering vector **S**, from the output configurations using the Debye formula [31] implemented by the software package debyer which is freely available on the internet (https://github.com/wojdyr/debyer). A Gaussian function was fitted to the structure factor peak to find the peak centre and the real space d-spacing corresponding to the structure factor peak was calculated as 1/S (as described above for the experimental WAXS results). This d-spacing can be related to the average spacing between the alkyl chains of the phospholipids.

3. Results and discussion

3.1. Wide angle X-ray scattering experiments

WAXS probes structures on the 1–10 Å length scale and so is ideal for studying the packing of lipid hydrocarbon chains. A pure fluid membrane typically shows a broad WAXS peak corresponding to approximately 4.6 Å (S = 0.22 $Å^{-1}$).

Fig. 1 shows the effect of pressure on the WAXS scattering from DMPC. Fig. 1a shows WAXS scattering patterns from pure DMPC at different pressures. At atmospheric pressure and 25 MPa, the broad scattering pattern indicates formation of a fluid bilayer structure. At 50 MPa, there is a small sharper peak at approximately 4.2 Å (S = 0.235 $Å^{-1}$) indicating coexistence of a lamellar gel phase. The coexistence of the original fluid phase is likely to be a kinetic effect

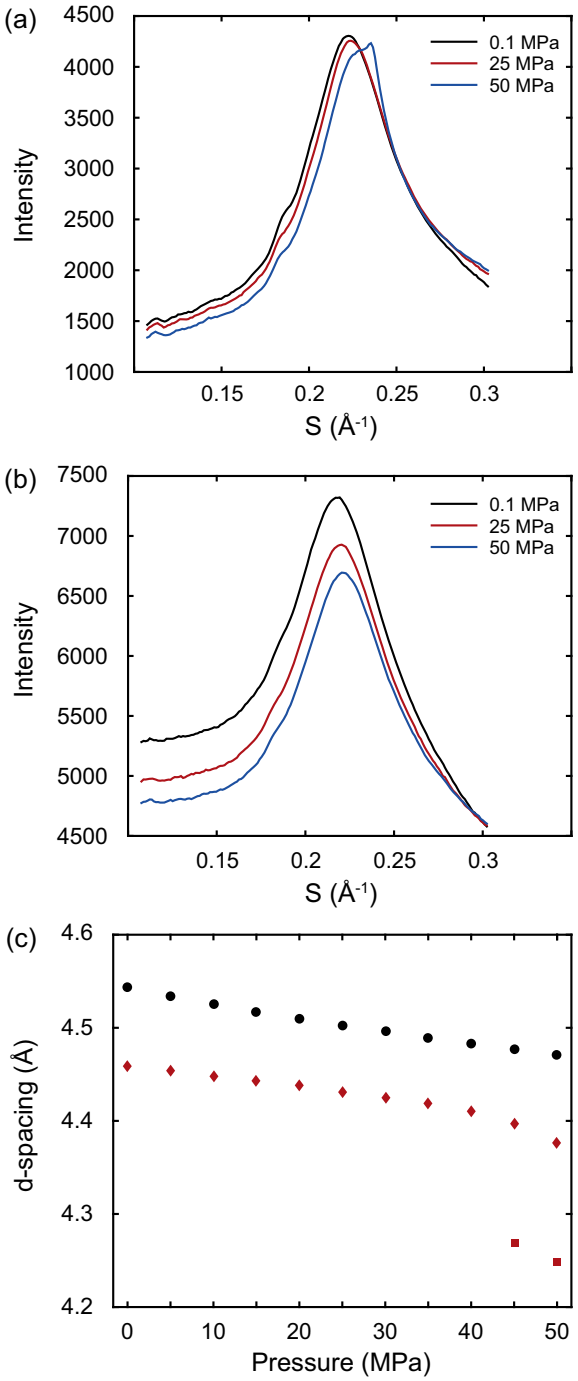

Fig. 1. Experimental data from WAXS experiments. The top panel shows scattering patterns from pure DMPC at 0.1 MPa (black), 20 MPa (red) and 40 MPa (blue). The middle panel shows scattering patterns from DMPC + halothane at 0.1 MPa (black), 20 MPa (red) and 40 MPa (blue). In these two panels, the peak moves to a higher S with increasing pressure. The bottom panel shows the d-spacing of the WAXS peak centre (related to the inter-alkyl chain spacing) of the phospholipids at different pressures, in the pure DMPC system (red diamonds) and in the DMPC/halothane system (black circles). The red squares show the co-existence of the gel phase with the fluid phase in pure DMPC at high pressures. (For interpretation of the references to colour in this figure legend, the reader is referred to the web version of this article.)

and if held at this pressure for an extended time, the membrane would transform fully to the gel phase. Fig. 1b shows corresponding scattering patterns for DMPC membranes containing halothane; the patterns appear very similar to those for pure DMPC, except that gel phase formation is suppressed within the pressure range studied, which is consistent with previous work showing an anaesthetic induced decrease in the gel transition temperature of lipid membranes [32]. Fig. 1c shows the change in the WAXS d-spacing with pressure. Increasing pressure causes a significant lateral compression of the membrane in both the pure DMPC membrane and those containing halothane. The d-spacing decreases by approximately 0.075 Å between atmospheric pressure and 50 MPa in both cases which is typical for a fluid membrane [33]. Halothane incorporation causes an increase in the d-spacing from 0.075 Å to 0.1 Å (approximately 2%) at all pressures studied, which is likely to be due to insertion of the halothane molecules between the lipid chains increasing the average chain spacing.

3.2. Molecular dynamics simulations

While X-ray scattering can provide a huge amount of information on the structure of membrane assemblies, the intrinsically low lateral ordering of fluid bilayers means that the resolution of WAXS is limited and it is difficult to extract atomic scale structural detail or probe specific molecular interactions. However, combining X-ray scattering with atomistic simulation offers the opportunity to probe two overlapping length scales and extract significantly more detailed information than would be available from experiments alone.

Table 1 shows the thermodynamic properties of the systems simulated by molecular dynamics. The energy and temperature are stable. The fluctuation of pressure is large due to the small size of the simulation box, which is typical for simulations of this scale.

The simulations give an area per DMPC molecule of $60.8\ Å^2 \pm 0.4\ Å^2$ at 0.1 MPa and $57.6\ Å^2 \pm 0.5\ Å^2$ at 40 MPa and 310 K. This agrees well with the experimentally determined values of $61.24\ Å^2 \pm 1.2\ Å^2$ [34] or $62.7\ Å^2$ [35], both at 303 K and 0.1 MPa. The change in area per lipid with pressure is highly consistent with the changes in chain spacing found experimentally above. It should be noted that while high pressures induce a reduction in the area per lipid, it is still significantly larger than that found for the gel phase of $47.51\ Å^2 \pm 0.13\ Å^2$ at 288 K [34], indicating that the membrane is in the fluid phase throughout all simulations (this is also confirmed by the calculated structure factors shown below).

Fig. 2 shows the position of the halothane C2 atoms and the DMPC choline nitrogen atoms relative to the bilayer mid-plane. The halothane preferentially occupies the region near the top of the hydrocarbon chains and the bilayer centre. Previous simulations with lower halothane concentrations [20] show less halothane at the bilayer mid-plane, but approximately the same concentration near the headgroup region as that found here. We believe that the bilayer mid-plane is effectively acting as a sink for excess halothane at these high concentrations.

Table 1
This table shows the thermodynamic properties of each system. E = total energy (kJ/mol), T = temperature (K), P = pressure (0.1 MPa).

System	E	T	P
Pure DMPC systems			
NPT 0.1 MPa	$-4.79 \times 10^4 \pm 561$	310 ± 2.54	2.03 ± 368
NPT 20 MPa	$-4.80 \times 10^4 \pm 452$	310 ± 2.48	188 ± 395
NPT 40 MPa	$-4.88 \times 10^4 \pm 560$	310 ± 2.64	403 ± 381
Halothane-DMPC systems			
NPT 0.1 MPa	$-4.49 \times 10^4 \pm 547$	310 ± 2.56	4.30 ± 368
NPT 20 MPa	$-4.53 \times 10^4 \pm 520$	310 ± 2.40	218 ± 367
NPT 40 MPa	$-4.58 \times 10^4 \pm 547$	310 ± 2.47	410 ± 367

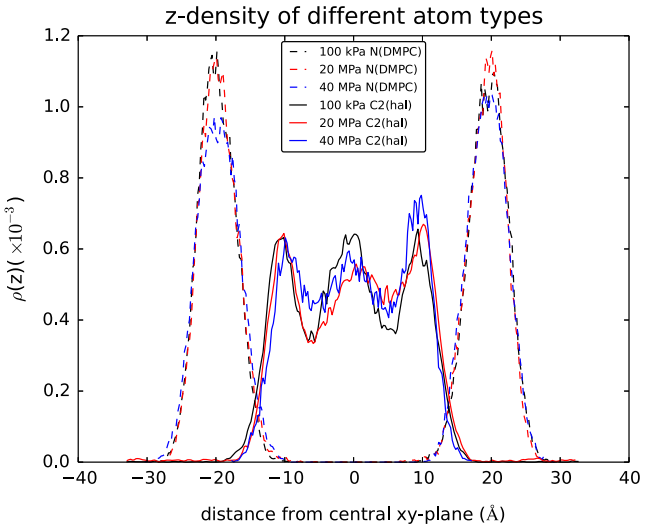

Fig. 2. Diagram showing the probability of finding a choline nitrogen atom from DMPC and a C2 atom of halothane along the depth of the membrane from simulations. The *z*-density for nitrogen has been reduced 64-fold for easy comparison.

Using the atomic coordinates from the simulations, we have calculated the lipid structure factor which is related to the expected X-ray scattering curve (although it should be noted that the two curves are not expected to be exactly the same). From these structure factor curves we have calculated a preferred hydrocarbon chain separation (equivalent to the WAXS d-spacing). Results from these calculations are shown in Fig. 3. Fig. 3a shows the structure factor calculated from the pure DMPC simulation data at different pressures, Fig. 3b shows corresponding structure factors from the DMPC/halothane simulation data. The bottom panel shows the corresponding d-spacing (calculated as for the experimental WAXS patterns) at different pressures; the d-spacing decreases monotonically as pressure increases. Simulations were carried out at atmospheric pressure, 20 MPa and 40 MPa and so the emerging gel phase observed in the experimental results is not expected here. While the absolute spacing values found from simulations are a little higher than those from experiment, the lateral expansion of the lipid chain packing on halothane incorporation and lateral compression behaviour with increasing pressure are reproduced well.

As mentioned previously, simulation data offers the important possibility of probing the structural behaviour of the lipid molecules that make up the membrane at atomic resolution, and of extracting structural parameters that would be extremely difficult to obtain by experiments alone. Fig. 4, shows the C–H bond order parameter of the DMPC alkyl chain going down the chain from the interfacial region to the bilayer mid-plane at 0.1 MPa and 40 MPa. The bond order parameter is given by

$$S_{CD} = \frac{3\cos^2\theta - 1}{2} \qquad (1)$$

where θ is the angle between the C–H bond and the membrane normal, and the angled brackets denote ensemble averaging over all the DMPC molecules, over the C atoms located at the same position in the two tails, and over all C–H bonds belonging to the same C atom. The order parameter gives information on the mobility of the hydrocarbon chain and the range of values of the parameter as defined here is $-1/2 \leqslant S_{CD} \leqslant 1$. When S_{CD} is nearer $-1/2$, the lipid main chain is more aligned with the membrane normal.

In pure DMPC, increasing the pressure causes a significant decrease in the order parameter (which corresponds to a decrease

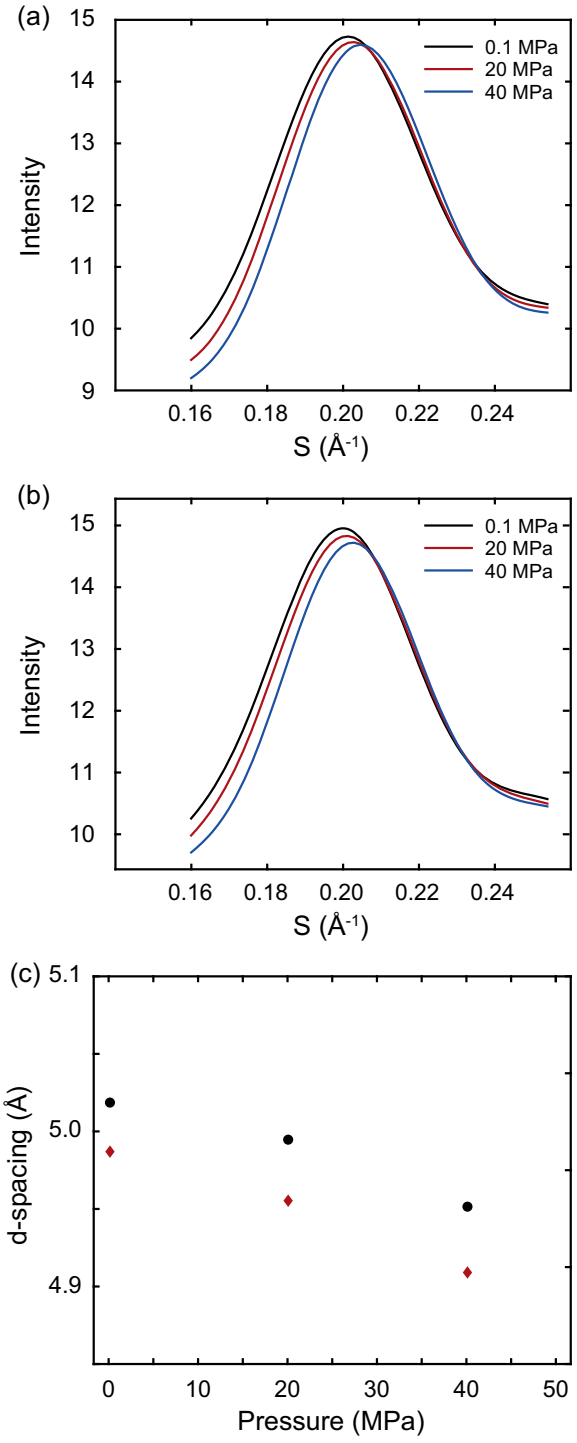

Fig. 3. Structure factor data calculated from molecular dynamics simulations. The top panel shows the structure factor calculated for pure DMPC at 0.1 MPa (black), 20 MPa (red) and 40 MPa (blue). The middle panel shows the structure factor calculated for DMPC + 33 halothane at 0.1 MPa (black), 20 MPa (red) and 40 MPa (blue). In these two panels, the peak moves to a higher S with increasing pressure. The bottom panel shows the d-spacing of the structure factor peak centre (related to inter-alkyl chain spacing) at different pressures, in the pure DMPC system (red diamonds) and in the DMPC/halothane system (black circles). (For interpretation of the references to colour in this figure legend, the reader is referred to the web version of this article.)

in conformational freedom) in the region between carbon atoms 3 and 6 while the rest of the chain remains relatively unaffected. In contrast, membranes with halothane incorporated show an

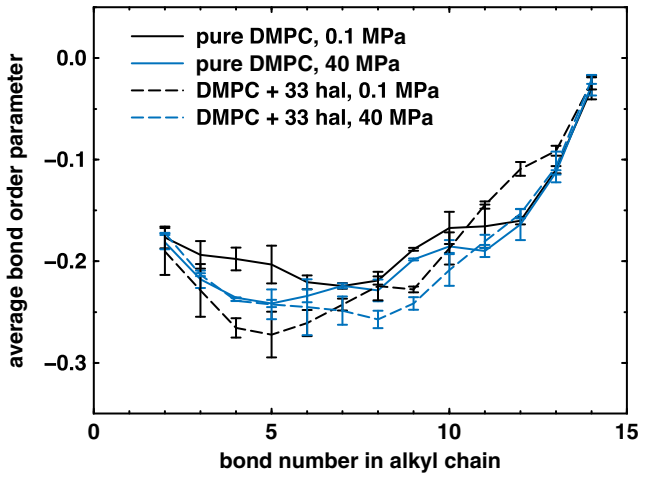

Fig. 4. Diagram showing the bond order parameter of the alkyl chain bonds. The number on the *x*-axis denotes the bond number, whilst the different lines denote the different conditions.

increase in order parameter in the carbon 3–6 region and a small decrease in order parameter further down the chain, this is likely to result from a change in the distribution of halothane through the membrane thickness. While this redistribution is not absolutely clear from Fig. 2, there does appear to be a small decrease in the halothane density at the bilayer mid-plane and a small increase in the halothane density nearer the membrane's hydrophobic - hydrophilic interface with increasing pressure.

Interestingly, incorporation of halothane at atmospheric pressure causes a significant reduction in the order parameter between carbon atoms 3 and 7. In contrast at 40 MPa, halothane has very little effect on this region of the chain, instead causing a small reduction in order parameter further down the chain. The effect of pressure and halothane incorporation on the order parameter of the upper section of the lipid hydrocarbon chain is summarised in Fig. 5 which shows that pressure progressively causes the order parameter for carbon 4 to converge for the pure DMPC and halothane containing simulation.

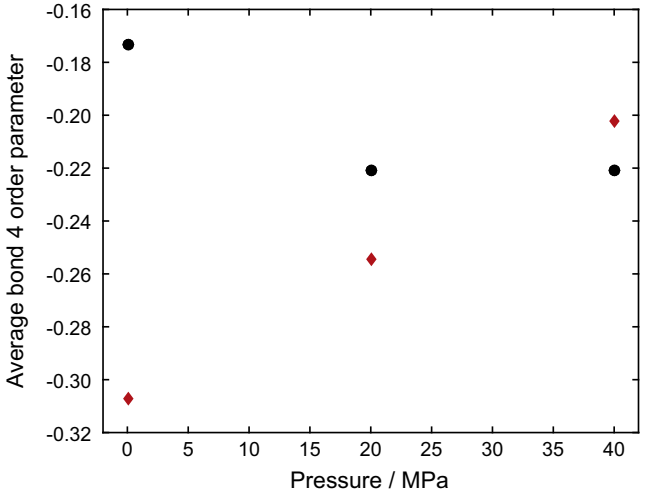

Fig. 5. Diagram showing the order parameter of bond 4. The black circles denote results from pure DMPC simulations, and the red diamonds denote results from simulations of DMPC/halothane systems. In the pure DMPC system, increasing the pressure decreases the S_{CD} of bond 4; in the DMPC/halothane system, increasing the pressure increases the S_{CD} of the same bond. (For interpretation of the references to colour in this figure legend, the reader is referred to the web version of this article.)

As mentioned above, there is a significant amount of evidence that general anaesthetics act at allosteric binding sites on specific transmembrane protein targets [15,36]. The structure of proteins is known to be significantly less sensitive to pressure than that of lipid membranes [37,38], however, the structure of transmembrane proteins are known to be highly sensitive to the structural properties of the lipid membrane in which they are incorporated [39]. The $GABA_A$ receptor is thought to be one of the most important of these proteins. Interestingly, site-directed mutagenesis experiments suggest that a possible important binding site for GA molecules is in the transmembrane domain of $GABA_A$ towards the interfacial region [15]. This corresponds to the area where we observe significant modulation of the membrane ordering by both halothane incorporation and pressure. In addition, recent experiments suggest that changes in the lateral structuring of membranes in response to anaesthetic incorporation and pressure may be important in modulating anaesthetic activity [40,41].

Our combined experimental-simulation approach offers a compelling molecular hypothesis for the pressure reversal of anaesthetics: pressure modulates the lateral structure of the lipid membrane in which target proteins are embedded and this may in turn disrupt the protein structure, changing the accessibility or dynamics of their GA binding sites.

4. Conclusion

The interaction of general anaesthetics and membranes have been studied for a long time. Previous experiments have shown that there is an interplay between anaesthetic effect and pressure. Cantor [42] suggested that drugs could induce lateral pressure change in the lipid membrane; these changes would shift the conformational equilibrium of membrane proteins and thus cause anaesthesia [43]. Scientists have certainly observed the effect of membrane on ion channel gating [44], but there still is a debate about the relative contributions of the membrane and the protein to general anaesthetic effects [45]. In this work, we used X-ray scattering to examine the structural properties of the membrane in the absence and presence of the general anaesthetic halothane, and at different pressures.

There have been very limited previous systematic scattering studies investigating the separation and structure of lipid chains under pressure. Braganza and Worcester [46] showed in a range of lipid membrane systems, that pressure causes a lateral compression of the hydrocarbon chains with a reduction in the chain separation of around 1.6–3.7% per 100 MPa. Here, we observe a lateral compression of the lipid hydrocarbon chains of approximately 3% per 100 MPa in experimental WAXS results and 3.5% per 100 MPa from simulations, both with and without halothane incorporated. At the same pressure, halothane alone causes an increase in the chain separation of about 2.2%.

Halothane and pressure both have a significant effect on the lateral ordering of lipid hydrocarbon chains. As mentioned above, there is significant evidence implicating small molecule/ membrane protein binding interactions in anaesthetic action and so we do not believe that changing the lipid packing within the membrane can directly explain pressure-induced anaesthetic reversal. However, it is possible that, at atmospheric pressure with halothane incorporated, the lipid membrane supports transmembrane protein structures that allow access to specific allosteric GA binding sites [44]; at elevated pressures, the membrane properties are altered which in turn may cause structural changes in the proteins responsible for GA action and if the anaesthetic binding pockets are modified, this could very conceivably modulate anaesthetic action. Additionally, it is possibile that pressure induced membrane structure changes could cause more subtle

modifications to the dynamics of the membrane protein: in this case, the GA binding may remain the same, but post-binding events could be altered, leading to a change in the functioning of the protein. Previous experiments have hinted at this possibility [47–50]. However, a lack of high-resolution experimental structure of these receptors, especially of $GABA_A$, has hampered progress in this area. We hope that in the near future, high-resolution membrane protein structures will become available which, in combination with our results will rapidly accelerate our understanding of the molecular mechanisms of general anaesthesia and its pressure reversal.

Acknowledgements

We thank Marcin Wojdyr for advice on his programme package debyer, Ruth Lynden-Bell and Jedrzej Wieteska for scientific discussions, and Stuart Rankin, Michael Rutter and Leung Hin-Tak for computational support. Simulations in this work were carried out on the Darwin Supercomputer of the University of Cambridge High Performance Computing Service using Strategic Research Infrastructure Funding from the Higher Education Funding Council for England. Experimental work was supported by UK Engineering and Physical Sciences Research Council (EPSRC) Programme Grant EP/J017566. We acknowledge Diamond Light Source for provision of synchrotron beamtime (SM6527 and SM9557) and we would like to thank Dr. Mark Tully and Dr. Andy Smith for their help with using beamline I22. All data created during this research are openly available from Imperial College London. Please see contact details at www.imperial.ac.uk/membranebiophysics; alternatively, the data can be obtained by contacting one of the authors at pc104@pasteur.fr.

References

[1] H. Meyer, Welche Eigenschaft des Anaesthetica bedingt ihre narkotische Wirkung?, Naunyn-Schmiedebergs Archiv für Experimentelle Pathologie und Pharmakologie 42 (1899) 109–118
[2] E. Overton, Studien über die Narkose zugleich ein Beitrag zur allgemeinen Pharmakologie, Gustav Fischer Verlag, Jena, Germany, 1901.
[3] F.H. Johnson, E.A. Flagler, Hydrostatic pressure reversal of narcosis in tadpoles, Science 112 (1950) 91–92.
[4] F.H. Johnson, E.A. Flagler, Activity of narcotized amphibian larvae under hydrostatic pressure, J. Cell. Compar. Physiol. 37 (1951) 15–25.
[5] M.J. Lever, K.W. Miller, W.D.M. Paton, E.B. Smith, Pressure reversal of anaesthesia, Nature 231 (1971) 368–371.
[6] K.W. Miller, W.D.M. Paton, R.A. Smith, E.B. Smith, The pressure reversal of general anesthesia and the critical volume hypothesis, Mol. Pharmacol. 9 (1973) 131–143.
[7] M.J. Halsey, B. Wardley-Smith, Pressure reversal of narcosis produced by anaesthetics, narcotics and tranquillisers, Nature 257 (1975) 811–813.
[8] A.F. Youngson, A.G. MacDonald, Interaction between halothane and hydrostatic pressure, Brit. J. Anaesth. 42 (1970) 801–802.
[9] S.A. Simon, J.L. Parmentier, P.B. Bennett, Anesthetic antagonism of the effects of high hydrostatic pressure on locomotory activity of the brine shrimp Artemia, Compar. Biochem. Physiol. 75A (1983) 193–199.
[10] J.R. Trudell, W.L. Hubbell, E.N. Cohen, The effect of two inhalation anesthetics on the order of spin-labeled phospholipid vesicles, Biochim. Biophys. Acta Biomembr. 291 (1973) 321–327.
[11] J.R. Trudell, W.L. Hubbell, E.N. Cohen, Pressure reversal of inhalation anesthetic-induced disorder in spin-labeled phospholipid vesicles, Biochim. Biophys. Acta Biomembr. 291 (1973) 328–334.
[12] N.P. Franks, General anaesthesia: from molecular targets to neuronal pathways of sleep and arousal, Nat. Rev. Neurosci. 9 (2008) 370–386.
[13] K. Herold, H. Hemmings, Sodium channels as targets for volatile anesthetics, Front. Pharmacol. 3 (2012) 50.
[14] C.M. Borghese, The molecular pharmacology of volatile anesthetics, Int. Anesthesiol. Clin. 53 (2015) 28–39.
[15] A. Jenkins, E.P. Greenblatt, H.J. Faulkner, E. Bertaccini, A. Light, A. Lin, A. Andreasen, A. Viner, J.R. Trudell, N.L. Harrison, Evidence for a common binding cavity for three general anesthetics within the $GABA_A$ receptor, J. Neurosci. 21 (2001) RC136.
[16] C.M. Borghese, J.A. Hicks, D.J. Lapid, J.R. Trudell, R.A. Harris, $GABA_A$ receptor transmembrane amino acids are critical for alcohol action: disulfide crosslinking and alkyl methanethiosulfonate labeling reveal relative location of binding sites, J. Neurochem. 128 (2014) 363–375.
[17] Y. Mokrab, V.N. Bavro, K. Mizuguchi, N.P. Todorov, I.L. Martin, S.M.J. Dunn, S.L. Chan, P.-L. Chan, Exploring ligand recognition and ion flow in comparative models of the human GABA type A receptor, J. Mol. Graph. Model. 26 (2007) 760–774.
[18] P.-L. Chau, P. Hoang, S. Picaud, P. Jedlovszky, A possible mechanism for pressure reversal of general anaesthetics from molecular simulations, Chem. Phys. Lett. 438 (2007) 294–297.
[19] P.-L. Chau, P. Jedlovszky, P. Hoang, S. Picaud, Pressure reversal of general anaesthetics: a possible mechanism from molecular dynamics simulations, J. Mol. Liq. 147 (2009) 128–134.
[20] K.M. Tu, N. Matubayasi, K.K. Liang, I.T. Todorov, S.L. Chan, P.-L. Chau, A possible molecular mechanism for the pressure reversal of general anaesthetics: aggregation of halothane in POPC bilayers at high pressure, Chem. Phys. Lett. 543 (2012) 148–154.
[21] J.R. Wieteska, P.R.L. Welche, K.-M. Tu, M. ElGamacy, G. Csanyi, M.C. Payne, P.-L. Chau, Isoflurane does not aggregate inside POPC bilayers at high pressure: implications for pressure reversal of general anaesthesia, Chem. Phys. Lett. 638 (2015) 116–121.
[22] J.E. Baenziger, S.E. Ryan, M.M. Goodreid, N.Q. Vuong, R.M. Sturgeon, C.J.B. daCosta, Lipid composition alters drug action at the nicotinic acetylcholine receptor, Mol. Pharmacol. 73 (2008) 880–890.
[23] C.J.B. daCosta, S.A. Medaglia, N. Lavigne, S.Z. Wang, C.L. Carswell, J.E. Baenziger, Anionic lipids allosterically modulate multiple nicotinic acetylcholine receptor conformation equilibria, J. Biol. Chem. 284 (2009) 33841–33849.
[24] P. Seeman, The membrane actions of anesthetics and tranquilizers, Pharmacol. Rev. 24 (1972) 583–655.
[25] N.J. Brooks, B.L.L.E. Gauthe, N.J. Terrill, S.E. Rogers, R.H. Templer, O. Ces, J.M. Seddon, Automated high pressure cell for pressure jump x-ray diffraction, Rev. Sci. Instrum. 81 (2010) 064103.
[26] J.C. Phillips, R. Braun, W. Wang, J. Gumbart, E. Tajkhorshid, E. Villa, C. Chipot, R. D. Skeel, L. Kalé, K. Schulten, Scalable molecular dynamics with NAMD, J. Comput. Chem. 26 (2005) 1781–1802.
[27] S.E. Feller, A.D. MacKerell, An improved empirical potential energy function for molecular simulations of phospholipids, J. Phys. Chem. B 104 (2000) 7510–7515.
[28] W.L. Jorgensen, J. Chandrasekhar, J.D. Madura, R.W. Impey, M.L. Klein, Comparison of simple potential functions for simulating liquid water, J. Chem. Phys. 79 (1983) 926–935.
[29] D. Scharf, K. Laasonen, Structure, effective pair potential and properties of halothane, Chem. Phys. Lett. 258 (1996) 276–282.
[30] S. Jo, J.B. Lim, J.B. Klauda, W. Im, CHARMM-GUI membrane builder for mixed bilayers and its application to yeast membranes, Biophys. J. 97 (2009) 50–58.
[31] P. Debye, Zerstreuung von Röntgenstrahlen, Ann. Phys. 351 (1915) 809–823.
[32] S. Kaneshina, H. Kamaya, I. Ueda, Thermodyanmics of pressure anesthetic antagonism on the phase transition of lipid membranes – displacement of anesthetic molecules, J. Colloid Interf. Sci. 93 (1983) 215–224.
[33] S. Purushothaman, P. Cicuta, O. Ces, N.J. Brooks, Influence of high pressure on the bending rigidity of model membranes, J. Phys. Chem. B 119 (30) (2015) 9805–9810.
[34] A.V. Hughes, S.J. Roser, M. Gerstenberg, A. Goldar, B. Stidder, R. Feidenhans'l, J. Bradshaw, Phase behavior of DMPC free supported bilayers studied by neutron reflectivity, Langmuir 18 (2002) 8161–8171.
[35] N. Kučerka, S. Tristram-Nagle, J.F. Nagle, Structure of fully hydrated fluid phase lipid bilayers with monosaturated chains, J. Membr. Biol. 208 (2005) 193–202.
[36] P.S. Garcia, S.E. Kolesky, A. Jenkins, General anesthetic actions on $GABA_A$ receptors, Curr. Neuropharmacol. 8 (2010) 2–9.
[37] R. Winter, C. Jeworrek, Effect of pressure on membranes, Soft Matter 5 (2009) 3157–3173.
[38] N.J. Brooks, Pressure effects on lipids and bio-membrane assemblies, IUCrJ 1 (2014) 470–477.
[39] K. Charalambous, P.J. Booth, R. Woscholski, J.M. Seddon, R.H. Templer, R.V. Law, L.M.C. Barter, O. Ces, Engineering de novo membrane-mediated protein – protein communication networks, J. Am. Chem. Soc. 134 (13) (2012) 5746–5749.
[40] B.B. Machta, E. Gray, M. Nouri, N.L.C. McCarthy, E.M. Gray, A.L. Miller, N.J. Brooks, S.L. Veatch, Conditions that stabilize membrane domains also antagonize n-alcohol anesthesia, Biophys. J. 111 (3) (2016) 537–545.
[41] S. Rukyilmaz, P.F. Almeida, S.L. Regen, Effects of isoflurane, halothane and chloroform on the interactions and lateral organization of lipids in the liquid-ordered phase, Langmuir 27 (2011) 14380–14385.
[42] R.S. Cantor, Lipid composition and the lateral pressure profile in bilayers, Biophys. J. 76 (1999) 2625–2639.
[43] D.K. Lee, D.J. Albershardt, R.S. Cantor, Exploring the mechanism of general anesthesia: kinetic analysis of $GABA_A$ receptor electrophysiology, Biophys. J. 108 (2015) 1081–1093.
[44] B. Martinac, J. Adler, C. Kung, Mechanosensitive ion channels of E. coli activated by amphipaths, Nature 348 (1990) 261–263.
[45] P.-L. Chau, New insights into the molecular mechanisms of general anaesthetics, Brit. J. Pharmacol. 161 (2010) 288–307.
[46] L.F. Braganza, D.L. Worcester, Structural changes in lipid bilayers and biological membranes caused by hydrostatic pressure, Biochemistry 25 (1986) 7484–7488.
[47] A. Angel, M.J. Halsey, B. Wardley-Smith, Interactions of γ-aminobutyric acid and noradrenaline in the high pressure neurological syndrome, Brit. J. Pharmacol. 79 (1983) 725–729.

[48] J.C. Rostain, B. Wardley-Smith, C. Forini, M.J. Halsey, Gamma-aminobutyric acid and the high pressure neurological syndrome, Neuropharmacology 25 (1986) 545–554.
[49] B. Kriem, B. Cagniard, C. Bouquet, J.-C. Rostain, J.H. Abraini, Modulation by GABA transmission in the substantia nigra compacta and reticulata of locomotor activity in rats exposed to high pressure, NeuroReport 9 (1998) 1343–1347.
[50] M.H. Millan, B. Wardley-Smith, M.J. Halsey, B.S. Meldrum, Brain nuclei and neurotransmitters involved in the regulation of the high pressure neurological syndrome in the rat, Neuropharmacology 30 (1991) 1351–1355.